Progress in multiscale computational electromagnetics in time domain

Luis Tobón[†,‡], **Jiefu Chen**[§], **Junho Lee**[*], **Mengqing Yuan**[*], **Bo Zhao**[*] and **Qing Huo Liu**[†]

[†]*Department of Electrical and Computer Engineering, Duke University, Durham, NC 27708, USA, e-mail: luis.tobonllano@duke.edu*

[‡]*Department of Electronic Engineering and Computer Science, Pontificia Universidad Javeriana-Cali, Santiago de Cali 56710, Colombia*

[§]*Adv. R&D Center, Weatherford International Ltd., Houston, TX 77060, USA*

[*]*Wave Computational Technology, Inc. (WCT), Durham, NC 27707, USA*

Abstract

Many system-level electromagnetic design problems are multiscale and very challenging to solve. They remain a significant barrier to system design optimization for a foreseeable future. Such multiscale problems often contain three electrical scales, i.e., the fine scale (geometrical feature size much smaller than a wavelength), the coarse scale (geometrical feature size greater than a wavelength), and the intermediate scale between the two extremes. Existing computational tools are based on single methodologies (such as finite element method or finite-difference time-domain method), and are unable to solve large multiscale problems. We will present our recent progress in solving realistic multiscale system-level EM design simulation problems in time domain. The discontinuous Galerkin time domain method is used as the fundamental framework for interfacing multiple scales with finite-element method, spectral element method, and finite difference method. Numerical results demonstrate significant advantages of our multiscale method. A more detail discussion of the method is given in [1].

Pulsed Electromagnetic Fields: Their Potentialities, Computation and Evaluation
I. E. Lager and L. J. Jiang (Eds.).
doi: 10.3233/978-1-61499-230-1-55

1 Introduction

Realistic system level electromagnetic problems such as electromagnetic interference (EMI), electromagnetic compatibility (EMC) ans signal integrity (SI) are often multiscale. Examples of multiscale problems include small devices under test in a reverberation chamber for EMC/EMI testing, and a multilayer package-to-chip structure in Fig. 1. Here electrically fine structures with details much smaller than a typical wavelength (mode stirrers, devices under testing in the chamber, or on-chip interconnects in the package-to-chip structure) coexist with electrically coarse structures comparable to or larger than a typical wavelength (the empty space insider the chamber, or the package in the multilayer circuit).

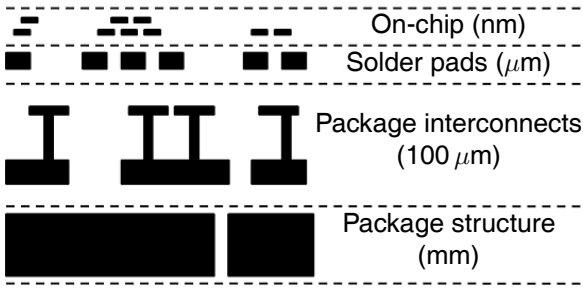

Figure 1: Multiscale package-to-chip structure.

Simulating transient multiscale problems can be very challenging for the conventional finite-difference time-domain (FDTD) method and the finite-element time-domain (FETD) method. The FDTD method [2, 3] requires an orthogonal grid. Thus, a high discretization density required to capture the geometric characteristics of electrically fine structures will lead to a large number of wasted unknowns in the electrically coarse domains. The subgridding technique [4] can alleviate this issue of the FDTD method; however, it will spoil the simple data structure of the standard FDTD scheme and greatly increase computational complexity. The FETD method [5,6] is more flexible in geometric modeling. However, this method requires solving matrix equations, either directly or iteratively. A discretized multiscale problem usually has a large number of unknowns, viz. huge system matrices. It can be prohibitively expensive to perform operations with huge matrices during time stepping.

Discontinuous Galerkin time-domain (DGTD) methods [7–17] are promising in solving multiscale problems. First, for geometric modeling, DGTD allows for domain decomposition. A multiscale structure can be divided into several subdomains, and each subdomain can be discretized by

a specific mesh density based on its geometric characteristics. Based on the idea of domain decomposition, DGTD is much more flexible than FDTD and FETD in modeling complex structures because large system matrices are split into a bunch of smaller matrices. DGTD can easily handle problems too large to be solved by the conventional FETD method. As for time integration, DGTD allows for different time stepping schemes to be used in different subdomains. For example, efficient explicit schemes can be applied to subdomains with coarser meshes and relatively large CFL numbers, while unconditionally stable implicit schemes can be employed in subdomains with dense meshes to overcome CFL restrictions. These flexibilities in both spatial and temporal discretization make DGTD efficient in multiscale simulations.

Constructing a DGTD system consists of several key steps: (a) deciding on which governing equations the DGTD method will be based on; (b) choosing element shape and corresponding basis functions for the spatial discretization of each subdomain; (c) applying numerical fluxes onto interfaces to stitch all subdomains together; and (d) selecting a time stepping scheme based on properties of a discretized system. Each step of the above procedure has more than one choice. Thus, dozens of DGTD variations have been proposed with different combinations of implementation schemes. In this review we provide a discussion of the fundamental issues of each step, emphasizing the details of one specific scheme based on mixed finite element discretization and the hybrid implicit-explicit (IMEX) time stepping scheme.

2 The discontinuous Galerkin system for transient electromagnetic analysis

2.1 Governing equations for time domain electromagnetic analysis

The transient electromagnetic problems can be governed by different equations such as first order Maxwell's equations or a second order wave equation. Mathematically these governing equations are equivalent, however, with different discretization schemes they differ greatly in numerical properties [18].

The second order wave equation uses directly curl-conforming elements [19–22], which are free of spurious modes and facilitate the imposition of boundary condition. Despite such advantages, the wave equations have difficulties in constructing the time-domain perfectly matched layer (PML), which is believed to be an all-purpose technique to truncate unbounded regions. Moreover, the implementation of numerical fluxes [23–25], a critical

step in building a DGTD system, is based on both $\boldsymbol{E}$ and $\boldsymbol{H}$ variables. These limitations make the wave equation with only one discretized field less suitable for DGTD methods.

To avoid the above difficulties the DGTD systems can be based on first order Maxwell's equations with both $\boldsymbol{E}$ and $\boldsymbol{H}$ as field variables

$$\epsilon\frac{\partial \boldsymbol{E}}{\partial t} + \sigma\boldsymbol{E} - \boldsymbol{\nabla}\times\boldsymbol{H} = -\boldsymbol{J}_{\mathrm{s}} \tag{1}$$

$$\mu\frac{\partial \boldsymbol{H}}{\partial t} + \boldsymbol{\nabla}\times\boldsymbol{E} = \boldsymbol{0} \tag{2}$$

In the following subsections we will see that it is straightforward to implement numerical fluxes for this first order system.

2.2 Galerkin's weak form and numerical fluxes

Denote $\boldsymbol{\Phi}$ and $\boldsymbol{\Psi}$ as basis functions for $\boldsymbol{E}$ and $\boldsymbol{H}$, respectively. With integration by parts, the Galerkin's weak forms of Maxwell's equations are

$$\begin{aligned}&\int_V \boldsymbol{\Phi}\cdot\left(\epsilon\frac{\partial \boldsymbol{E}}{\partial t} + \sigma\boldsymbol{E} + \boldsymbol{J}_{\mathrm{s}}\right)\mathrm{d}V - \int_V (\boldsymbol{\nabla}\times\boldsymbol{\Phi})\cdot\boldsymbol{H}\,\mathrm{d}V\\ &= \int_S \boldsymbol{\Phi}\cdot(\boldsymbol{n}\times\boldsymbol{H})\,\mathrm{d}S\end{aligned} \tag{3}$$

$$\begin{aligned}&\int_V \boldsymbol{\Psi}\cdot\mu\frac{\partial \boldsymbol{H}}{\partial t}\mathrm{d}V + \int_V (\boldsymbol{\nabla}\times\boldsymbol{\Psi})\cdot\boldsymbol{E}\,\mathrm{d}V\\ &= -\int_S \boldsymbol{\Psi}\cdot(\boldsymbol{n}\times\boldsymbol{E})\,\mathrm{d}S\end{aligned} \tag{4}$$

where V denotes the volume of a subdomain, which contains one or more elements, $\boldsymbol{n}$ is the unit normal vector located on surface S and pointing to the outside of V. The terms on the right hand sides of equations (3) and (4) are integrals over subdomain interfaces. In DGTD methods they are evaluated by numerical fluxes.

Choosing different numerical fluxes can lead to different DGTD systems. One commonly used numerical flux is the Riemann solver [23, 24], which is a type of upwind numerical flux and is derived from the physical process of wave propagation and reflection across an interface between two different media

$$\begin{aligned}\int_S \boldsymbol{\Phi}\cdot(\boldsymbol{n}\times\boldsymbol{H})\,\mathrm{d}S = &\int_S \boldsymbol{\Phi}\cdot\left[\boldsymbol{n}\times\frac{Z^{(i)}\boldsymbol{H}^{(i)} + Z^{(j)}\boldsymbol{H}^{(j)}}{Z^{(i)}+Z^{(j)}}\right]\mathrm{d}S\\ &+\int_S \boldsymbol{\Phi}\cdot\left[\boldsymbol{n}\times\boldsymbol{n}\times\frac{\boldsymbol{E}^{(i)}-\boldsymbol{E}^{(j)}}{Z^{(i)}+Z^{(j)}}\right]\mathrm{d}S\end{aligned} \tag{5}$$

$$\int_S \boldsymbol{\Psi} \cdot (\boldsymbol{n} \times \boldsymbol{E})\,\mathrm{d}S = \int_S \boldsymbol{\Psi} \cdot \left[\boldsymbol{n} \times \frac{Y^{(i)}\boldsymbol{E}^{(i)} + Y^{(j)}\boldsymbol{E}^{(j)}}{Y^{(i)} + Y^{(j)}}\right] \mathrm{d}S - \int_S \boldsymbol{\Psi} \cdot \left[\boldsymbol{n} \times \boldsymbol{n} \times \frac{\boldsymbol{H}^{(i)} - \boldsymbol{H}^{(j)}}{Y^{(i)} + Y^{(j)}}\right] \mathrm{d}S \tag{6}$$

where $Z^{(i)} = 1/Y^{(i)} = \sqrt{\mu^{(i)}/\epsilon^{(i)}}$ and $Z^{(j)} = 1/Y^{(j)} = \sqrt{\mu^{(j)}/\epsilon^{(j)}}$ are wave impedances for the i-th and the j-th subdomains, respectively.

2.3 Discretized system of linear equations

Assuming a multiscale structure is divided into N subdomains, the discretized system of equations by the DGTD method will be

$$\boldsymbol{M}_{ee}^{(i)} \frac{\mathrm{d}\boldsymbol{e}^{(i)}}{\mathrm{d}t} = \boldsymbol{K}_{eh}^{(i)} \boldsymbol{h}^{(i)} + \boldsymbol{C}_{ee}^{(i)} \boldsymbol{e}^{(i)} + \boldsymbol{j}^{(i)} + \sum_{j=1}^{N} \left(\boldsymbol{L}_{ee}^{(ij)} \boldsymbol{e}^{(j)} + \boldsymbol{L}_{eh}^{(ij)} \boldsymbol{h}^{(j)} \right), \quad i = 1, \ldots, N \tag{7}$$

$$\boldsymbol{M}_{hh}^{(i)} \frac{d\boldsymbol{h}^{(i)}}{dt} = \boldsymbol{K}_{he}^{(i)} \boldsymbol{e}^{(i)} + \sum_{j=1}^{N} \left(\boldsymbol{L}_{he}^{(ij)} \boldsymbol{e}^{(j)} + \boldsymbol{L}_{hh}^{(ij)} \boldsymbol{h}^{(j)} \right), \quad i = 1, \ldots, N \tag{8}$$

where $\boldsymbol{e}^{(i)}$ and $\boldsymbol{h}^{(i)}$ are vectors of the discretized electric and magnetic fields, $\boldsymbol{M}_{ee}^{(i)}$ and $\boldsymbol{M}_{hh}^{(i)}$ are the mass matrices, $\boldsymbol{C}_{ee}^{(i)}$ is the damping matrix, $\boldsymbol{K}_{eh}^{(i)}$ and $\boldsymbol{K}_{he}^{(i)}$ are the stiffness matrices, and $\boldsymbol{j}^{(i)}$ is vector of the discretized excitations of the i-th subdomain. Matrices $\boldsymbol{L}_{ee}^{(ij)}$, $\boldsymbol{L}_{eh}^{(ij)}$, $\boldsymbol{L}_{he}^{(ij)}$, $\boldsymbol{L}_{hh}^{(ij)}$ are obtained from the interface integrations and can be viewed as the couplings between fields of the i-th and j-th subdomains. Detailed formulations of these vectors and matrices are referred to [26].

3 Spatial discretization with different basis functions

3.1 DG-FETD: discontinuous Galerkin finite-element time-domain method

The discontinuous Galerkin finite-element time-domain (DG-FETD) method is a very popular DGTD scheme with finite elements employed for spatial discretization of subdomains. The DG-FETD method can be viewed

as a combination of discontinuous Galerkin method (DGM) and finite element method (FEM) in time domain. All kinds of finite elements, e.g., nodal or edge elements as basis functions, tetrahedral, prism, or hexahedral elements as element shapes, have been used in constructing different DG-FETD schemes [7–15].

3.2 DG-SETD: discontinuous Galerkin spectral-element time-domain method

Despite its meshing flexibility, the lower order DG-FETD scheme suffers from a slow convergence rate and a large numerical dispersion. To make multiscale simulations more efficient, the electrically coarse part can be selected out and discretized by higher order finite elements with a coarser mesh. The spectral elements are special types of higher order finite elements with interpolation points chosen based on spectral polynomials, such as Gauss-Lobatto-Legendre (GLL) polynomials [27, 28]. By doing so the spectral elements will avoid the Runge phenomenon and lead to diagonal or block diagonal mass matrices, which are especially favorable to time domain computations because inversion of such mass matrices becomes trivial.

4 Time stepping schemes

For a DGTD system, time stepping can be performed subdomain by subdomain rather than solving a huge matrix system as in FETD schemes. This advantage of DGTD methods can save a large amount of memory during time stepping, and furthermore, it makes parallel computation straightforward for a DGTD system.

Local time stepping and hybrid implicit-explicit schemes for multiscale simulations

A discretized multiscale DGTD system usually contains electrically coarse subdomains with coarse meshes, which have relatively large CFL numbers when an explicit time integration scheme is used. Meanwhile the multiscale system also contains electrically fine subdomains with dense meshes, whose CFL numbers may be several orders smaller than those of electrically coarse subdomains. Local time stepping methods such as the multirate Adams-Bashforth scheme [29,30] or hybrid implicit-explicit schemes [31] can be a good fit for a DGTD system under this circumstance.

Take the hybrid implicit-explicit Runge-Kutta (IMEX-RK) [32] scheme

as an example, which consists of two parts. The first part is the explicit Runge-Kutta (ERK) method

$$\begin{array}{c|ccccc} 0 & 0 & 0 & \dots & \dots & 0 \\ c_2 & a^{\text{ex}}_{2,1} & 0 & \ddots & \ddots & \vdots \\ c_3 & a^{\text{ex}}_{3,1} & a^{\text{ex}}_{3,2} & 0 & \ddots & \vdots \\ \vdots & \vdots & \vdots & \vdots & \ddots & 0 \\ c_s & a^{\text{ex}}_{s,1} & a^{\text{ex}}_{s,2} & \dots & a^{\text{ex}}_{s,s-1} & 0 \\ \hline & b_1 & b_2 & b_3 & \dots & b_s \end{array} \tag{9}$$

The second part is for the explicit singly diagonally implicit Runge-Kutta (ESDIRK) method

$$\begin{array}{c|ccccc} 0 & a^{\text{im}}_{1,1} & 0 & \dots & \dots & 0 \\ c_2 & a^{\text{im}}_{2,1} & a^{\text{im}}_{2,2} & 0 & \ddots & \vdots \\ c_3 & a^{\text{im}}_{3,1} & a^{\text{im}}_{3,2} & a^{\text{im}}_{3,3} & \ddots & \vdots \\ \vdots & \vdots & \vdots & \vdots & \ddots & 0 \\ c_s & a^{\text{im}}_{s,1} & a^{\text{im}}_{s,2} & \dots & a^{\text{im}}_{s,s-1} & a^{\text{im}}_{s,s} \\ \hline & b_1 & b_2 & b_3 & \dots & b_s \end{array} \tag{10}$$

Assuming a discretized multiscale problem contains N_{ex} explicit subdomains and N_{im} implicit subdomains, the time stepping formulation for the i-th subdomain based on IMEX-RK with s stages is

$$\boldsymbol{v}^{(i)}_{n+1} = \boldsymbol{v}^{(i)}_n + \Delta t \sum_{k=1}^{s} b_k \boldsymbol{u}^{(i)}_k, \quad i = 1, \cdots, N_{\text{im}} + N_{\text{ex}} \tag{11}$$

where

$$\begin{aligned} \boldsymbol{M}^{(i)} \boldsymbol{u}^{(i)}_k = & \sum_{j=N_{\text{im}}+1}^{N_{\text{im}}+N_{\text{ex}}} \boldsymbol{L}^{(ij)} \left(\boldsymbol{v}^{(j)}_n + \Delta t \sum_{l=1}^{k-1} a^{\text{ex}}_{k,l} \boldsymbol{u}^{(j)}_l \right) \\ & + \sum_{j=1}^{N_{\text{im}}} \boldsymbol{L}^{(ij)} \left(\boldsymbol{v}^{(j)}_n + \Delta t \sum_{l=1}^{k} a^{\text{im}}_{k,l} \boldsymbol{u}^{(j)}_l \right) + \boldsymbol{f}^{(i)}(t_n + c_k \Delta t) \end{aligned} \tag{12}$$

for explicit subdomains, and

$$\begin{aligned} \left(\boldsymbol{M}^{(i)} - \Delta t a^{\text{im}}_{k,k} \boldsymbol{L}^{(ii)} \right) \boldsymbol{u}^{(i)}_k = & \boldsymbol{f}^{(i)} \left(t_n + c_k \Delta t \right) + \boldsymbol{L}^{(ii)} \left(\boldsymbol{v}^{(i)}_n + \Delta t \sum_{l=1}^{k-1} a^{\text{im}}_{k,l} \boldsymbol{u}^{(j)}_l \right) \\ & + \sum_{j=N_{\text{im}}+1}^{N_{\text{im}}+N_{\text{ex}}} \boldsymbol{L}^{(ij)} \left(\boldsymbol{v}^{(j)}_n + \Delta t \sum_{l=1}^{k-1} a^{\text{ex}}_{k,l} \boldsymbol{u}^{(j)}_l \right) \end{aligned} \tag{13}$$

for implicit subdomains.

The hybrid IMEX scheme does not need temporal interpolation at the interfaces between explicit and implicit regions. To our understanding, the hybrid IMEX scheme is very desirable for a DGTD system with well separated CFL numbers, while the local time stepping scheme may be more suitable for a DGTD system with CFL numbers spanning continuously from a very small value to a relatively large one.

5 Conclusions

In this paper we have reviewed some important concepts, formulations, and implementations of discontinuous Galerkin time domain schemes for multiscale electromagnetic simulations, in particular, the mixed finite element discretization and the hybrid implicit-explicit (IMEX) time stepping scheme. Numerical examples demonstrate that the proposed method is a promising time-domain technique for simulating multiscale structures.

Bibliography

[1] J. Chen, and Q. H. Liu, "Discontinuous Galerkin time domain methods for multiscale electromagnetic simulations: A review," *Proc. IEEE*, in press, 2013.

[2] K. Yee, "Numerical solution of initial boundary value problems involving Maxwell's equations in isotropic media," *IEEE Trans. Antennas Propagat.*, vol. 14, no. 3, pp. 302–307, May 1966.

[3] A. Taflove and S. C. Hagness, *Computational Electrodynamics: The Finite-Difference Time-Domain Method*, 3rd edition, Boston: Artech House, Inc., 2005.

[4] C. Sun and C. W. Trueman, "Three-dimensional subgridding algorithm for FDTD," *IEEE Trans. Antennas Propagat.*, vol. 45, no. 3, pp. 422–429, March 1997.

[5] A. Cangellaris, C. Lin, and K. Mei, "Point-matched time domain finite element methods for electromagnetic radiation and scattering," *IEEE Trans. Antennas Propagat.*, vol. 35, no. 10, pp. 1160–1173, Oct. 1987.

[6] J. F. Lee and Z. Sacks, "Whitney elements time domain (WETD) methods," *IEEE Trans. Magn.*, vol. 31, no. 3, pp. 1325–1329, May 1995.

[7] B. Cockburn, F. Li, and C. W. Shu, "Locally divergence-free discontinuous Galerkin methods for the Maxwell equations," *J. Comput. Phys.*, vol. 194, no. 2, pp. 588–610, March 2004.

[8] Q. H. Liu and G. Zhao, "Advances in PSTD techniques." Chapter 17, in *Computational Electromagnetics: The Finite-Difference Time-Domain Method*, A. Taflove and S. C. Hagness, Ed., Boston: Artech House, Inc., 2005.

[9] T. Xiao and Q. H. Liu, "Three-dimensional unstructured-grid discontinuous Galerkin method for Maxwell's equations with well-posed perfectly matched layer," *Microw. Opt. Techn. Lett.*, vol. 46, no. 5, pp. 459–463, Sept. 2005.

[10] J. S. Hesthaven, and T. Warburton, "Nodal high-order methods on unstructured grids: I. time-domain solution of Maxwell's equations," *J. Comput. Phys.*, vol. 181, no. 1, pp. 186–221, Sept. 2002.

[11] G. C. Cohen, X. Ferrieres, and S. Pernet, "A spatial high-order hexahedral discontinuous Galerkin method to solve Maxwell's equations in time domain," *J. Comput. Phys.*, vol. 217, no. 2, pp. 340–363, Sept. 2006.

[12] F. Q. Hu, M. Y. Hussaini, and P. Rasetarinera, "An analysis of the discontinuous Galerkin method for wave propagation problems," *J. Comput. Phys.*, vol. 151, no. 2, pp. 921–946, May 1999.

[13] J. S. Hesthaven and T. Warburton, *Nodal Discontinuous Galerkin Methods*, New York, NY: Springer, 2008.

[14] S. Gedney, C. Luo, J. Roden, R. Crawford, B. Guernsey, J. Miller, T. Kramer, and E. W. Lucas, "The discontinuous Galerkin finite-element time-domain method of Maxwell's equations," *ACES Journal*, vol. 24, no. 2, pp. 129–142, April 2009.

[15] H. Fahs and S. Lanteria, "A high-order non-conforming discontinuous Galerkin method for time-domain electromagnetics," *J. Comput. Phys.*, vol. 234, no. 4, pp. 1088–1096, June 2010.

[16] J. S. Hesthaven and T. C. Warburton, "Nodal high-order methods on unstructured grids - 1. Time-domain solution of Maxwell's equations," *J. Comput. Phys.*, vol. 181, no. 1, pp. 186–221, Sept. 2002.

[17] J. H. Lee, J. Chen, and Q. H. Liu, "A 3-D discontinuous spectral element time-domain method for Maxwell's equations," *IEEE Trans. Antennas Propag.*, vol. 57, no. 9, pp. 2666–2674, Sept. 2009.

[18] N. Marais and D. B. Davidson, "Numerical evaluation of high-order finite element time domain formulations in electromagnetics," *IEEE Trans. Antennas Propag.*, vol. 56, no. 12, pp. 3743–3751, Dec. 2008.

[19] J. C. Nédélec, "Mixed finite elements in $\mathbb{R}^3$," *Numer. Math.*, vol. 35, no. 3, pp. 315–341, Sept. 1980.

[20] A. Bossavit, "A rationale for 'edge-elements' in 3-D fields computations," *IEEE Trans. Magn.*, vol. 24, no. 1, pp. 74–79, Jan. 1988.

[21] A. F. Peterson, S. L. Ray, and R. Mittra, *Computational Methods for Electromagnetics*, IEEE Press, 1998.

[22] J. Jin, *The Finite Element Method in Electromagnetics*, 2nd edition, New York, NY: John Wiley & Sons, Inc., 2002.

[23] V. Shankar, A. H. Mohammadian, and W. F. Hall, "A time-domain, finite-volume treatment for the Maxwell equations," *Electromagnetics*, vol. 10, no. 1, pp. 127–145, Jan. 1990.

[24] A. H. Mohammadian, V. Shankar, and W. F. Hall, "Computation of electromagnetic scattering and radiation using a time-domain finite-volume discretization procedure," *Comput. Phys. Commun.*, vol. 68, no. 1–3, pp. 175–196, Nov. 1991.

[25] E. Montseny, S. Pernet, X. Ferrieres, and G. Cohen, "Dissipative terms and local time-stepping improvements in a spatial high order discontinuous Galerkin scheme for the time-domain Maxwell's equations," *J. Comput. Phys.*, vol. 227, no. 14, pp. 6795–6820, Jul. 2008.

[26] J. Chen, L. E. Tobon, M. Chai, J. A. Mix, and Q. H. Liu, "Efficient implicit-explicit time stepping scheme with domain decomposition for multiscale modeling of layered structures," *IEEE Trans. Compon., Packag., Manuf. Technol.*, vol. 1, no. 9, pp. 1438–1446, Sept. 2011.

[27] G. Cohen and M. Durufle, "Non-spurious spectral like element methods for Maxwell's equations," *J. Comput. Math.*, vol. 25, no. 3, pp. 282–300, 2007.

[28] J. H. Lee and Q. H. Liu, "An efficient 3-D spectral element method for Schrödinger equation in nanodevice simulation," *IEEE Trans. Comput.-Aided Design Integr. Circuits Syst.*, vol. 24, no. 12, pp. 1848–1858, Dec. 2005.

[29] S. Piperno, "Symplectic local time-stepping in non-dissipative DGTD methods applied to wave propagation problems," *ESAIM-Math. Model. Num.*, vol. 40, no. 5, pp. 815–841, Sept. 2006.

[30] S. Schomann, N. Godel, T. Warburton, and M. Clemens, "Local timestepping techniques using Taylor expansion for modeling electromagnetic wave propagation with discontinuous Galerkin-FEM," *IEEE Trans. Magn.*, vol. 46, no. 8, pp. 3504–3507, Aug. 2010.

[31] A. Kanevsky, M. H. Carpenter, D. Gottlieb, and J. S. Hesthaven, "Application of implicit-explicit high order Runge-Kutta methods to discontinuous-Galerkin schemes," *J. Comput. Phys.*, vol. 225, no. 2, pp. 1753–1781, Aug. 2007.

[32] J. C. Butcher, *Numerical Methods for Ordinary Differential Equations*, New York, NY: John Wiley & Sons, Inc., 2003.